CWP-493
May 2005

Migration/Inversion:
Think Image Point Coordinates, Process in Acquisition Surface Coordinates

Norman Bleisteiin*, Yu Zhang†, Sheng Xu†,
Guanquan Zhang‡ & Samuel H. Gray§

*Center for Wave Phenomena, Department of Geophysics, Colorado School of Mines, Golden, CO 80401

†Veritas DGC Inc., 10300 Town Park Drive, Houston, TX 77072

‡Institue of Computational Mathematics & Sci/Eng. Computing, Academy of Mathematics & System Sciences, Chinese Academy of Sciences, Beijing, 100080, P. R. China

§Veritas DGC Inc., 715 Fifth Avenue SW, Calgary, Alberta, Canada T2P 5A2

Center for Wave Phenomena
Colorado School of Mines
Golden, Colorado 80401
(303)273-3557

Migration/Inversion: Think Image Point Coordinates, Process in Acquisition Surface Coordinates

Norman Bleistein,[1] Yu Zhang,[2] Sheng Xu,[2] Guanquan Zhang,[3] and Samuel H. Gray[4]

Abstract

We state a general principle for seismic migration/inversion (M/I) processes: think image point coordinates; compute in surface coordinates. This principle allows the natural separation of multiple travel paths of energy from a source to a reflector to a receiver. Further, the Beylkin determinant (Jacobian of transformation between processing parameters and acquisition surface coordinates) is particularly simple in stark contrast to the common-offset Beylkin determinant in standard single-arrival Kirchhoff M/I.

A feature of this type of processing is that it changes the deconvolution structure of Kirchhoff M/I operators or the deconvolution imaging operator of wave equation migration into convolution operators; that is, division by Green's functions is replaced by multiplications by adjoint Green's functions.

This transformation from image point coordinates to surface coordinates is also applied to a recently developed extension of the standard Kirchhoff inversion method. The standard method uses WKBJ Green's functions in the integration process and tends to produce more imaging artifacts than alternatives, such as methods using Gaussian beam representations of the Green's functions in the inversion formula. These methods point to the need for a true-amplitude Kirchhoff technique that uses more general Green's functions: Gaussian beams, true-amplitude one-way Green's functions, or Green's functions from the two-way wave eqation. Here, we present a derivation of a true-amplitude Kirchhoff M/I that uses these more general Green's functions. When this inversion is recast as an integral over all sources and receivers, the formula is surprisingly simple.

1 Introduction

Xu et al [2001] presented a 2D Kirchhoff inversion formula as an integral of input reflection data over all possible dip angles at an image point for each fixed value of the opening-(or scattering-) angle between the rays from source and receiver at an image point. They then recast the result as an integral over source and receiver points on the acquisition surface. Bleistein and Gray [2002] presented a 3D version of that formula. The transformation

[1]Center for Wave Phenomena, Department of Geophysics, Colorado School of Mines, Golden, CO 80401-1887, USA

[2]Veritas DGC Inc., 10300 Town Park Drive,Houston, TX 77072, USA

[3]Institute of Computational Mathematics & Sci/Eng. Computing, Academy of Mathematics & System Sciences, Chinese Academy of Sciences, Beijing, 100080, P. R. China

[4]Veritas DGC Inc., 715 Fifth Avenue SW, Suite 2200 Calgary, Alberta, Canada T2P 5A2

normalization factor of the final Kirchhoff inversion with the chosen Green's functions. If we did not use this approximation, then we would need to carry out a pointwise six-fold integration for the purposes of normalization of the amplitude of the kernel.

An important concept about true-amplitude processing is at work here. "True amplitude" as applied to the output of an inversion algorithm refers to estimation of plane wave reflection coefficients. For anything but plane-wave reflection from planar reflectors in a homogeneous medium, this is a WKBJ-approximate estimate and has little or no meaning in the context of full wave-form solutions of the wave equation. Thus, although we image better with better Green's functions, reflection coefficients are estimated via ray-theoretic asymptotic solutions. Hence, the normalization factors need to be no better than what is provided by ray theory, while the general Green's functions used in the extended algorithm are expected to be numerically close to the WKBJ Green's function when they are evaluated away from caustics and other anomalies. Thus, we contend that there is both heuristic and physical justification for this simplification.

This full wave form Kirchhoff inversion also benefits from starting with a formula that is an integration over angular variables at the image point and transforming to source/receiver coordinates. When this is done, the WKBJ normalization is no longer explicit in the inversion formula. Ray theory is used in this final result only to sort the output into panels defined by common-opening-angle/common-azimuth-angle (COA/CAA) of the rays at the image point.

To summarize, if we start with a Kirchhoff M/I in migration dip coordinates, the transformation to surface coordinates can be applied. As in the more classical Kirchhoff M/I, this will produce an output that is separated into COA/CAA gathers. The result of that transformation on this Kirchhoff M/I with more general Green's functions is described here, as well.

Kirchhoff inversion of data gathered from parallel lines of multi-streamer data is both particularly important and particularly elusive. In 3D, the classical Kirchhoff inversion applies to data sets defined by two spatial parameters that characterize the source/receiver distribution. So for example, one might think of common-offset data in which the two parameters define the midpoint between source and receiver at a fixed azimuth (compass direction) on the acquisition surface, or one might think of common-shot data in which the source point is fixed and the two parameters describe the receiver location. Each shot of a multi-streamer survey "looks like" a common-shot data set, except that the data acquisition in the orthogonal direction to the streamer set is too narrow for common-shot M/I. Thus, it is necessary to use data from all of the shots to generate an inversion output. Consequently, we must work with a four spatial parameter data set: two parameters for each source location and two parameters for each receiver location. Kirchhoff inversion as sums over all sources and receivers, as presented here, provides such an inversion. We are not aware of any other Kirchhoff inversion that applies to this type of data acquisition.

We present results in order of progressing complexity. We begin with a discussion of the recent result for true amplitude WEM where a summation over angle (in 2D) or angle pair (in 3D) is transformed to summation over acquisition surface source coordinate(s). We then consider Kirchhoff inversion in image-point coordinates and describe the transformation to source and receiver coordinates. Finally, we discuss the extension of Kirchhoff inversion to

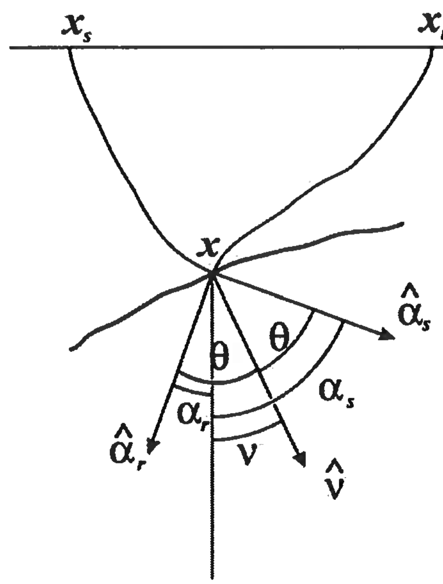

Figure 1:

Coordinates of the 2D inversion process. $\boldsymbol{x}$; the image point. $\boldsymbol{x}_s$ and $\boldsymbol{x}_r$; source and specular receiver, respectively. θ; incident specular angle of the source ray, also the reflection angle with respect to the normal. $\hat{\boldsymbol{\alpha}}_s$ and $\hat{\boldsymbol{\alpha}}_r$; unit vectors along the specular rays from the image point to the source and receiver, respectively. $\hat{\boldsymbol{\nu}}$, migration dip; also at specular, unit normal to the reflector. α_s, α_r, ν; angles with respect to the vertical of the vectors $\hat{\boldsymbol{\alpha}}_s$, $\hat{\boldsymbol{\alpha}}_r$, $\hat{\boldsymbol{\nu}}$.

Kirchhoff inversion formula for common shot data given by Bleistein et al [2001].[2] In turn, this reference contains a proof that the output has a peak value on the reflector proportional to an angularly dependent reflection coefficient (angle θ) at the specular angle (for which Snell's law is satisfied by the ray directions at the image point).

In the application, we have to contend with the issue of discretization in the estimate of $R(\boldsymbol{x}, \theta)$. We expect that noise due to discretization and truncation can be attenuated by averaging over nearby values of incidence angle around the given incidence angle, all at the same image point. Therefore we propose to average over a set of angles near a particular incidence angle θ. Varying the incidence angle at the image point is equivalent—via a mapping by rays—to varying the source point at the upper surface; that is, varying the incidence angle is equivalent to varying the shot and data set to which the WEM is applied.

[2]The reader familiar with Kirchhoff inversion might find it mysterious that this formula – an integral over frequency – could agree with a Kirchhoff migration formula, which is an integral over frequency and receivers. The connection becomes clearer when $p_U(\boldsymbol{x}_r, \boldsymbol{x}_s, \boldsymbol{x}, \omega)$ is replaced by its Green's function representation in terms of the observed data at the upper surface, that is, $p_U(\boldsymbol{x}_r, \boldsymbol{x}_s, \boldsymbol{x}, \omega) = \int p_U(\boldsymbol{x}_r, \boldsymbol{x}_s, \boldsymbol{x}'_r \omega) A(\boldsymbol{x}'_r, \boldsymbol{x}) \exp\{i\omega\tau(\boldsymbol{x}'_r, \boldsymbol{x})\} d\boldsymbol{x}'_r$. That representation is a convolution over receivers, restoring the double integral character of Kirchhoff M/I.

where * denotes complex conjugate.

We remark that the interval $(\theta - \Delta\theta/2, \theta + \Delta\theta/2)$, centered at θ, does not map into a symmetric interval in sources about the central source $x_s(\theta)$. Below, we will denote the interval in source coordinates by $(x_s - \Delta_-, x_s + \Delta_+)$.

By using $d\theta'$ as defined in Equation (3) in the reflectivity-averaging equation, Equation (2), we find that

$$\overline{R(\boldsymbol{x},\theta)} = \frac{4}{\Delta\theta}\int d\omega \int_{x_s-\Delta_-}^{x_s+\Delta_+} A(\boldsymbol{x}_s',\boldsymbol{x})A^*(\boldsymbol{x}_s',\boldsymbol{x})\,\frac{\cos\beta_s'}{v(\boldsymbol{x}_s')}\,\frac{p_U(\boldsymbol{x}_r,\boldsymbol{x}_s',\boldsymbol{x},\omega)}{p_D(\boldsymbol{x}_s',\boldsymbol{x},\omega)}\,dx_s' \tag{4}$$

In this equation, θ on the left side and $\boldsymbol{x}_s$ in the limits of integration on the right are connected by the ray that propagates from the image point to $\boldsymbol{x}_s$.

Recall that the concept of "true amplitude" makes sense only when the image is produced by a single arrival and certain asymptotic approximations are valid. One of those approximations is

$$A(\boldsymbol{x}_s,\boldsymbol{x})A^*(\boldsymbol{x}_s,\boldsymbol{x}) \approx p_D(\boldsymbol{x}_s,\boldsymbol{x},\omega)p_D^*(\boldsymbol{x}_s,\boldsymbol{x},\omega). \tag{5}$$

Using this approximation in the averaged reflectivity of Equation (4) yields

$$\overline{R(\boldsymbol{x},\theta)} = \frac{4}{\Delta\theta}\int d\omega \int_{x_s-\Delta_-}^{x_s+\Delta_+} \frac{\cos\beta_s'}{v(\boldsymbol{x}_s')}\,\overline{p}_D(\boldsymbol{x}_s',\boldsymbol{x},\omega)p_U(\boldsymbol{x}_r,\boldsymbol{x}_s',\boldsymbol{x},\omega)\,dx_s'. \tag{6}$$

Comparing the right side here with the right side of the reflectivity definition, Equation (1), we see that a deconvolution-type imaging formula has been recast as a correlation-type imaging formula by averaging over incidence angles at the image point and then transforming that angular integral into an integral over source locations at the upper surface.

We remark that whether we compute the averaged reflectivity from Equation (2), which is an integral over dip angle, or from Equation (6), which is an integral over sources, it is necessary to compute ray trajectories from the upper surface to the image point. Equation (6) would seem to require a further calculation of an image interval $(x_s - \Delta_-, x_s + \Delta_+)$ from the interval $(\theta - \Delta\theta/2, \theta + \Delta\theta/2)$.

As an alternative, we propose the following procedure to compute the averages over all θ-intervals. Decompose the θ-domain into intervals of length $\Delta\theta$. For each input trace–that is, for each source/receiver pair–determine the angle θ' and the angle β_s'. Calculate the integrand and add it to a running sum in the appropriate θ-interval. For sufficiently small $\Delta\theta$, even if there is multi-pathing, the separate trajectories from source to image point will produce values of θ that are separated by more than the width $2\Delta\theta$ that defines the bin size. This method accumulates the average reflectivity for all θ intervals simultaneously.

We note further that the first representation of the averaged reflectivity, Equation (2), has an alternative interpretation. It is the discrete form of the seemingly redundant distributional equation

$$R(\boldsymbol{x},\theta) = \frac{1}{2\pi}\int d\omega \int \frac{p_U(\boldsymbol{x}_r,\boldsymbol{x}_s,\boldsymbol{x},\omega)}{p_D(\boldsymbol{x}_s,\boldsymbol{x},\omega)}\delta(\theta-\theta')d\theta'. \tag{7}$$

In transforming from this result back to the discrete form of the averaged-reflectivity in Equation (2), $\Delta\theta$ is the "weight" of the discrete approximation to the delta-function and the integral yields an estimate of the distributional integral over the interval of length $\Delta\theta$.

we find that

$$\sin\theta' d\theta' d\phi' = 16\pi^2 v(\boldsymbol{x}) A(\boldsymbol{x}_s, \boldsymbol{x}) A^*(\boldsymbol{x}_s, \boldsymbol{x}) \frac{\cos\beta'_{s1}}{v(\boldsymbol{x}_s)} dx_{s1} dx_{s2}. \tag{9}$$

Here, β'_s is the angle between the ray direction (or normal to the ray-tube cross-section) and the normal to differential source area cross-section. Equation (9) should be compared with the differential $d\theta'$, Equation (3), which is the appropriate angular differential in 2D. Substituting the expression for the differential angular area element of Equation (9) into the averaged reflectivity result, Equation (8), leads to

$$\overline{R(\boldsymbol{x}, \theta, \phi)} = \frac{8\pi}{|\Omega|} \int d\omega \int_\Delta v(\boldsymbol{x}) p_{_D}^*(\boldsymbol{x}_s, \boldsymbol{x}, \omega) p_{_U}(\boldsymbol{x}_r, \boldsymbol{x}_s, \boldsymbol{x}, \omega) \frac{\cos\beta'_{s1}}{v(\boldsymbol{x}_s)} dx_{s1} dx_{s2}. \tag{10}$$

In this equation, Δ is the image on the acquisition surface of the angle domain Ω in θ' and ϕ'.

As in 2D, we do not propose determining the domain Δ in Equation (10). Instead, we discretize the angular domain on the unit sphere of directions defined by θ and ϕ. For each source/receiver pair, we accumulate the integrand into running sums in the appropriate θ, ϕ subdomain as discussed above for the 2D case.

The 3D averaged reflectivity defined by Equation (8) has a distributional interpretation similar to the equivalence between the 2D reflectivity average, Equation (2), and its distributional equivalent, Equation (7). The correct identity arises from the observation that

$$1 = \frac{1}{|\Omega|} \int_\Omega \sin\theta' d\theta' d\phi' = \int_\Omega \delta(\theta - \theta') \delta(\sin\theta'(\phi - \phi')) \sin\theta' d\theta' d\phi' = \int_\Omega \delta(\theta - \theta') \delta(\phi - \phi') d\theta' d\phi' \tag{11}$$

Here, $d\theta'$ and $\sin\theta' d\phi'$ are differential arc length variables in the polar and azimuthal directions, respectively; hence, the second equality. The third equality then follows from the distributional identity succinctly stated as $|a|\delta(ax) = \delta(x)$. In this case, the reflectivity average defined by Equation (8) is a discretization of the distributional form of the reflectivity expressed in either of the following two forms:

$$\begin{aligned} R(\boldsymbol{x}, \theta, \phi) &= \frac{1}{2\pi} \int d\omega \int_\Omega \frac{p_{_U}(\boldsymbol{x}_r, \boldsymbol{x}_s, \boldsymbol{x}, \omega)}{p_{_D}(\boldsymbol{x}_s, \boldsymbol{x}, \omega)} \delta(\theta - \theta') \delta(\sin\theta'(\phi - \phi')) \sin\theta' d\theta' d\phi' \\ &= \frac{1}{2\pi} \int d\omega \int_\Omega \frac{p_{_U}(\boldsymbol{x}_r, \boldsymbol{x}_s, \boldsymbol{x}, \omega)}{p_{_D}(\boldsymbol{x}_s, \boldsymbol{x}, \omega)} \delta(\theta - \theta') \delta(\phi - \phi') d\theta' d\phi'. \end{aligned} \tag{12}$$

As before, these seemingly redundant identities allow us to transform between integrals in image domain angular coordinates and integrals in surface coordinates by proceeding with the change of variables described above.

2.2 Observations

The pattern of the discussion here will be repeated in the following sections. The objective is to transform integrals in image point angular variables to acquisition surface variables. The

Figure 3 to the source and receiver coordinates, respectively. Here we go one step further, expressing those Jacobians in terms of the 3D WKBJ amplitudes of the ray theoretic Green's functions connecting the image point with the source and receiver point, respectively.

Our starting point is Equation (26) of Bleistein and Gray. However, that result was equivalent to the reflectivity β of Bleistein et al [2001], equation (5.1.21). Here we prefer to use the equivalent of β_1 (not to be confused with the dip angle β_s of Figure 2), given by equation (5.1.47) in the same reference, but rewritten in terms of the variables of this paper.

Remark

The reflectivity function β yields a reflectivity map whose peak value on a reflector is

$$\beta^{\text{peak}} = R(\boldsymbol{x}, \theta, \phi) \frac{\cos\theta}{2\pi v(\boldsymbol{x})} \int F(\omega) d\omega.$$

In this equation, R is the geometrical optics or plane wave reflection coefficient at the specular reflection angles θ and ϕ, $v(\boldsymbol{x})$ is the wave speed, and $F(\omega)$ is the source signature. On the other hand, β_1 yields a reflectivity map whose peak value on the reflector is

$$\beta_1^{\text{peak}} = R(\boldsymbol{x}, \theta, \phi) \frac{1}{2\pi} \int F(\omega) d\omega.$$

The reflectivity β is a scaled band limited delta function in space with dimension $1/\mathsf{LENGTH}$, while β_1 is a scaled band limited delta function in time with dimension $1/\mathsf{TIME}$, both under the assumption that the source signature given by $F(\omega)$ is dimensionless. Both functions are scaled by the geometrical optics reflection coefficient but they differ by a factor of $\cos\theta/v(\boldsymbol{x})$. Thus, the quotient provides an estimate of the cosine of the specular reflection angle. Parenthetically (off the subject of this paper), in tests of numerical accuracy of this method, our experience is that the percentage error in the estimates of $\cos\theta$ are typically an order of magnitude smaller than the the error in the estimate of the reflection coefficient itself. We explain this by the fact that the integrands for these two reflectivity operators differ by only one factor and we expect that their errors will trend in the same direction. Consequently, when we examine the quotient that produces the estimate of $\cos\theta/v(\boldsymbol{x})$, the form of this quotient is

$$\frac{\cos\theta}{v(\boldsymbol{x})} \cdot \frac{1+\epsilon_1}{1+\epsilon_2} \approx \frac{\cos\theta}{v(\boldsymbol{x})} \cdot [1 + \epsilon_1 - \epsilon_2 + \cdots],$$

with ϵ_1 and ϵ_2 *having the same sign.* That is, the fractional error in the quotient turns about to be approximately the magnitude of the difference of the fractional errors of the two separate integrals and thereby smaller in magnitude than either of the separate errors.

End remark

relates the discrete average over a patch on the unit sphere to a distributional integral over the same patch.

We have now prepared the inversion formula for transformation to source and receiver variables. As described in the outline at the end of the previous section, this transformation is done in stages. With reference to the variables depicted in Figure 3, we first transform from ν_1, ν_2, θ', ϕ' to α_{s1}, α_{s2}, α_{r1}, α_{r2} and then transform these variables to surface variables through ray Jacobians. This derivation is carried out in Appendix C. Using the result Equation (C-5) from the appendix in the representation Equation (15) for the reflectivity as an integral over four angles at the image point leads to

$$\mathcal{R}(\boldsymbol{x},\theta,\phi) = 32\pi^2 v(\boldsymbol{x}) \int \frac{\cos\beta_s}{v(\boldsymbol{x}_s)} \frac{\cos\beta_r}{v(\boldsymbol{x}_r)} D_3(\boldsymbol{x},\boldsymbol{x}_r,\boldsymbol{x}_s) \tag{16}$$

$$\cdot A^*(\boldsymbol{x}_s,\boldsymbol{x})A^*(\boldsymbol{x}_r,\boldsymbol{x})\delta(\theta'-\theta)\delta(\sin\theta'(\phi'-\phi))dx_{s1}dx_{s2}dx_{r1}dx_{r2}.$$

In this equation, as in the previous section, θ', ϕ', β_s and β_r are all functions of the integration variables defined through the changes of variables. In the computation, these angles are measured by ray tracing from the source and receiver point to the image point. Thus, there is no need to define them explicitly in terms of the integration variables.

In practice, this integral will be carried out discretely. To do so, we replace each of the delta functions with a discrete approximation and then restrict the domain of integration to cover the support of the discrete delta functions (domain of nonzero values of the discrete delta functions). Therefore, let us set

$$\delta(\theta-\theta') \approx \begin{cases} \dfrac{1}{\Delta\theta}, & \theta-\Delta\theta/2 \le \theta' \le \theta+\Delta\theta/2 \\ 0, & \text{otherwise.} \end{cases},$$

$$\delta(\sin\theta'(\phi-\phi')) \approx \begin{cases} \dfrac{1}{\sin\theta\Delta\phi}, & \phi-\Delta\phi/2 \le \phi' \le \phi+\Delta\phi/2 \\ 0, & \text{otherwise.} \end{cases}.$$

The dual range $(\theta-\Delta\theta/2, \theta+\Delta\theta/2, \phi-\Delta\phi/2, \phi+\Delta\phi/2)$ defines a domain on the unit sphere, Ω, with area $|\Omega| = \sin\theta\Delta\theta\ \Delta\phi$. We denote the image of Ω under the mapping by rays to the upper surface as the range Δ. Then the discrete version of Equation (16) for the reflectivity function as an integral over all sources and receivers is

$$\overline{\mathcal{R}(\boldsymbol{x},\theta,\phi)} = \frac{32\pi^2 v(\boldsymbol{x})}{|\Omega|} \int_\Delta \frac{\cos\beta_{s1}}{v(\boldsymbol{x}_s)} \frac{\cos\beta_{r1}}{v(\boldsymbol{x}_r)} D_3(\boldsymbol{x},\boldsymbol{x}_r,\boldsymbol{x}_s) \tag{17}$$

$$\cdot A^*(\boldsymbol{x}_s,\boldsymbol{x})A^*(\boldsymbol{x}_r,\boldsymbol{x})dx_{s1}dx_{s2}dx_{r1}dx_{r2}.$$

Here, we are justified introducing the overbar $\overline{\mathcal{R}}$ because the result again has the form of an average.

4 Full wave form Kirchhoff-approximate modeling and inversion

We change directions at this point to describe an extension of Kirchhoff modeling and inversion using full wave form Green's functions. We remind the reader that for us "true amplitude" is meant in an asymptotic (ray-theoretic) sense. In forward modeling, that means that the wavefield is well-approximated by one or a sum of WKBJ contributions, with traveltime determined by the eikonal equation, amplitude determined by the transport equation, and with a possible additional phase shift adjustments provided by the KMAH index.

For inversion, we have already described "true amplitude" to mean an output that has peak value proportional to the WKBJ plane-wave reflection coefficient. This is predicted by the theory only when the image is generated by a single specular ray trajectory from source to image point to receiver. When there are multiple arrivals, the image is created by an overlay of contributions from specular source/receiver pairs with different reflection coefficients. At such points, it is not important what the weighting is, except that it have the right order of magnitude for balancing with the output from other image points.

After deriving the full wave form Kirchhoff inversion formula, we will specialize it to inversion in migration dip angles, thereby connecting this new result to the theory presented in the earlier sections.

The basic steps in the method are as follows.

(1) Start from the Kirchhoff approximation as a volume integral, but use any form of Green's function, as suggested above. In this form of the Kirchhoff approximation, the reflectivity function appears explicitly under the integral sign and the output is (synthetic) model data for any source/receiver pair.

(2) View this representation as a modeling operator operating on the reflectivity function. Write down a pseudo-inverse operator on the data to obtain an inversion for the reflectivity.

(3) Use asymptotics to simplify the operator, but preserve the more general Green's functions where ever possible so as not to destroy the central character of the degree of imaging quality of the inversion.

4.1 Kirchhoff modeling

The forward modeling Kirchhoff approximation is derived in Appendix D. The new feature here is that the result uses full wave form Green's functions. For example, we could use Green's functions generated by Gaussian beams, solutions of true amplitude one-way wave equations or solutions of the two-way wave equation. Furthermore, we write the Kirchhoff approximation as a *volume* integral, rather than a surface integral. This is now fairly standard when the forward model is used in inversion theory.

The upward reflected wavefield from a source $\boldsymbol{x}_s$ measured at a receiver $\boldsymbol{x}_r$ is

$$u_R(\boldsymbol{x}_r, \boldsymbol{x}_s, \omega) \sim -i\omega F(\omega) \int_S \mathcal{R}_0(\boldsymbol{x}', \theta, \phi) |\nabla_{\boldsymbol{x}'}\phi| G_s(\boldsymbol{x}', \boldsymbol{x}_s, \omega) G_r(\boldsymbol{x}_r, \boldsymbol{x}', \omega) dV. \tag{18}$$

In this equation,

$$\|(K^{\dagger}K)^{-1}\| = \left|\int d^2\xi\omega^2 d\omega \int dV |\nabla_x \phi(\boldsymbol{x},\boldsymbol{\xi})| G_s^*(\boldsymbol{x}_s,\boldsymbol{x},\omega) G_r^*(\boldsymbol{x},\boldsymbol{x}_r,\omega) \right. \tag{22}$$

$$\left. \cdot |\nabla_y \phi(\boldsymbol{x}',\boldsymbol{\xi})| G_s(\boldsymbol{x}',\boldsymbol{x}_s,\omega) G_r(\boldsymbol{x}_r,\boldsymbol{x}',\omega)\right|^{-1},$$

with

$$\tau(\boldsymbol{x},\boldsymbol{\xi}) = \tau(\boldsymbol{x},\boldsymbol{x}_s) + \tau(\boldsymbol{x},\boldsymbol{x}_r), \quad \tau(\boldsymbol{x}',\boldsymbol{\xi}) = \tau(\boldsymbol{x}',\boldsymbol{x}_s) + \tau(\boldsymbol{x}',\boldsymbol{x}_r). \tag{23}$$

4.3 Analysis of the pseudo-inverse norm $\|(K^{\dagger}K)^{-1}\|$

Clearly, we do not want to carry out the six-fold integral of the norm indicated in the definition Equation (22). Fortunately, it is not necessary to do so. As noted above, accurate "amplitude" in standard Kirchhoff inversion has relevance only when the image is created by a single arrival. Therefore we might as well replace this norm by its asymptotic expansion under the assumption that there is only a single arrival. That is accomplished by using ray theory to approximate the Green's functions in the integrand of Equation (22) that defines the norm $\|(K^{\dagger}K)^{-1}\|$: all of the more accurate Green's functions have the same ray-theoretic approximation, consistent with the underlying full wave equation. This is an important principle that is fundamental to extracting amplitude information from inversion processes with more general Green's functions than those provided by WKBJ.

Asymptotic analysis of this norm then leads to a calculation almost identical to the one used to derive the Kirchhoff inversion in the first place. The details are carried out in Appendix E. The final result is

$$\|(K^{\dagger}K)^{-1}\| = \frac{1}{8\pi^3}\frac{|h(\boldsymbol{x},\boldsymbol{\xi})|}{|\nabla_x\tau(\boldsymbol{x},\boldsymbol{\xi})|^2}\frac{1}{|A_s(\boldsymbol{x},\boldsymbol{x}_s)A_r(\boldsymbol{x}_r,\boldsymbol{x})|^2}. \tag{24}$$

In this equation, $h(\boldsymbol{x},\boldsymbol{\xi})$ is the Beylkin determinant defined by equation Equation (E-4).

4.4 Full wave form Kirchhoff Inversion

Next, we use the approximation in Equation (24) in the representation, Equation (21), for $\mathcal{R}_0(\boldsymbol{x},\theta,\phi)$ to obtain

$$\mathcal{R}_0(\boldsymbol{x},\theta,\phi) = \frac{1}{8\pi^3}\int \frac{G_s^*(\boldsymbol{x}_s,\boldsymbol{x},\omega)G_r^*(\boldsymbol{x},\boldsymbol{x}_r,\omega)}{|A_s(\boldsymbol{x},\boldsymbol{x}_s)A_r(\boldsymbol{x}_r,\boldsymbol{x})|^2}\frac{|h(\boldsymbol{x},\boldsymbol{\xi})|}{|\nabla_x\tau(\boldsymbol{x},\boldsymbol{\xi})|} i\omega u_R(\boldsymbol{x}_r,\boldsymbol{x}_s,\omega)d\omega d^2\xi. \tag{25}$$

When the Green's functions here are replaced by their ray-theoretic approximations, this formula reduces to the general inversion formula for β in Bleistein et al [2001], equation (5.1.21). This assures us that the reflectivity function produces the reflection coefficient times the bandlimited singular function of the reflector (with dimension 1/LENGTH) when

4.5 Full wave form inversion in migration angular coordinates recast as an integral in source/seceiver coordinates.

We are now prepared to connect full wave form Kirchhoff inversion to the theme of the earlier sections of the paper. As a first step, we specialize the last two representations of the reflectivity to the case where ξ_1 and ξ_2 are just the polar angles ν_1 and ν_2 used in the earlier sections of the paper. In this case, one can check that

$$\left|\frac{\partial \hat{\nu}}{\partial \xi_1} \times \frac{\partial \hat{\nu}}{\partial \xi_2}\right| = \left|\frac{\partial \hat{\nu}}{\partial \nu_1} \times \frac{\partial \hat{\nu}}{\partial \nu_2}\right| = \sin \nu_1. \tag{31}$$

Now, the reflectivity as defined by Equation (28) and Equation (30) become

$$\mathcal{R}(\boldsymbol{x},\theta,\phi) = \frac{1}{8\pi^3}\int \frac{G_s^*(\boldsymbol{x}_s,\boldsymbol{x},\omega)G_r^*(\boldsymbol{x},\boldsymbol{x}_r,\omega)}{|A_s(\boldsymbol{x},\boldsymbol{x}_s)A_r(\boldsymbol{x}_r,\boldsymbol{x})|^2}\left[\frac{2\cos\theta}{v(\boldsymbol{x})}\right] i\omega u_R(\boldsymbol{x}_r,\boldsymbol{x}_s,\omega)d\omega \sin\nu_1 d\nu_1 d\nu_2, \tag{32}$$

and

$$\mathcal{R}(\boldsymbol{x},\theta,\phi) = \frac{1}{8\pi^3}\int \frac{1}{G_s(\boldsymbol{x}_s,\boldsymbol{x},\omega)G_r(\boldsymbol{x},\boldsymbol{x}_r,\omega)}\left[\frac{2\cos\theta}{v(\boldsymbol{x})}\right] i\omega u_R(\boldsymbol{x}_r,\boldsymbol{x}_s,\omega)d\omega \sin\nu_1 d\nu_1 d\nu_2, \tag{33}$$

respectively.

Equation (32) should be compared to the Kirchhoff inversion, Equation (13), derived using WKBJ Green's functions, observing that in Equation (13)

$$\frac{1}{|A_s(\boldsymbol{x},\boldsymbol{x}_s)A_r(\boldsymbol{x}_r,\boldsymbol{x})|^2}\sin\nu_1 d\nu_1 d\nu_2 = \frac{1}{A_s^*(\boldsymbol{x},\boldsymbol{x}_s)A_r^*(\boldsymbol{x}_r,\boldsymbol{x})}\frac{1}{A_s(\boldsymbol{x},\boldsymbol{x}_s)A_r(\boldsymbol{x}_r,\boldsymbol{x})}\sin\nu_1 d\nu_1 d\nu_2.$$

Equation (13) was recast as an integral over source/receiver coordinates in Equation (16). In that process, the factors

$$\frac{1}{4\pi^2}\frac{2\cos\theta}{v(\boldsymbol{x})}\frac{1}{A(\boldsymbol{x},\boldsymbol{x}_s)A(\boldsymbol{x},\boldsymbol{x}_r)}\sin\nu_1 d\nu_1 d\nu_2$$

were replaced by

$$16\pi\frac{\cos\beta_{s1}}{v(\boldsymbol{x}_s)}\frac{\cos\beta_{r1}}{v(\boldsymbol{x}_r)}\frac{v(\boldsymbol{x})}{\sin\theta'}A^*(\boldsymbol{x}_s,\boldsymbol{x})A^*(\boldsymbol{x}_r,\boldsymbol{x})\delta(\theta'-\theta)\delta(\phi'-\phi)dx_{s1}dx_{s2}dx_{r1}dx_{r2}.$$

Thus, we can recast the full wave form reflectivity in Equation (32) as an integral over source/receiver coordinates by making the same replacements in this reflectivity formula. That is,

$$\begin{aligned}\mathcal{R}(\boldsymbol{x},\theta,\phi) = 16\pi v(\boldsymbol{x})\int & G_s^*(\boldsymbol{x}_s,\boldsymbol{x},\omega)G_r^*(\boldsymbol{x},\boldsymbol{x}_r,\omega) i\omega u_R(\boldsymbol{x}_r,\boldsymbol{x}_s,\omega)d\omega \\ & \cdot \frac{\cos\beta_s}{v(\boldsymbol{x}_s)}\frac{\cos\beta_r}{v(\boldsymbol{x}_r)}\delta(\theta'-\theta)\delta(\sin\theta'(\phi'-\phi))dx_{s1}dx_{s2}dx_{r1}dx_{r2}.\end{aligned} \tag{34}$$

4 The general inversion formula that resulted was then specialized to using the image point migration dip polar angles as the variables of integration and recasting the result as an integral over sources and receivers.

This process led to Equation (35) for full wave form reflectivity as an integral over all sources and receivers resulting in an output in COA/CAA panels. This is a correlation-type inversion formula.

Use of the full wave form Green's functions in the Kirchhoff approximation and then use of their WKBJ approximations in the estimate of the magnitude of the normal operator both depend on the basis of "true-amplitude" Kirchhoff inversion. Our ultimate objective as regards amplitude is an estimate of the non-normal incidence plane wave reflection coefficient at each point on the reflector. This coefficient is generalized via ray theory from plane waves incident on planar reflectors in homogeneous media to curved wave fronts incident on curved reflectors in heterogeneous media. As such, the concept only has meaning when we can speak of single arrivals at the reflector in media whose length scales allow the WKBJ wave form to make sense. Thus, the interchange between full wave form Green's functions and their WKBJ approximations wherever amplitude issues are concerned also makes sense; we do no better at reflection amplitude estimates when we use the full wave form Green's functions than when we use their WKBJ approximations. However, the full wave form Green's functions do provide better image quality.

5 Summary and Conclusions.

We have considered three approaches to migration/inversion, namely WEM, traditional Kirchhoff migration, and an extension of the Kirchhoff method to full wave form imaging. In the first case, integration of image point angle(s) was introduced as an averaging process. In the second and third cases, we wrote the Kirchhoff M/I process as an integration over image point angles. In each of these cases, we recast the integrals over angles as integrals over the source/receiver coordinates. This procedure produced imaging/inversion formulas written as integrations over all sources and receivers. (Although we have only considered horizontal acquisition surfaces here, the extension to curved acquisition surfaces is straightforward, as noted in item 3 in the discussion at the end of Section 2.) We have also described how the processing can be organized to lead to output in common opening angle, common azimuth angle at the image point.

For data gathered over parallel lines of multi-streamer cables, Kirchhoff inversion is particularly elusive. However, the Kirchhoff inversions presented in the previous two sections can be applied to these data. We are not aware of any other Kirchhoff inversion for this type of survey.

The full wave form Kirchhoff inversion of the previous section is also of recent derivation. The only elements of the full wave form inversion formula Equation (35) are only appropriate propagators, the differentiated observed data in the frequency domain, and dip-correction factors at the upper surface.

Zhang, Y., Zhang, G., and Bleistein, N., 2003, True amplitude wave equation migration arising from true amplitude one-way wave equations: Inverse Problems, 19, 1113-1138.

Zhang, Y., Zhang, G., and Bleistein, N., 2004a, Theory of True Amplitude One-way Wave Equations and True Amplitude Common-shot Migration: Geophysics, submitted.

Zhang, Y., Xu, S., Zhang, G., and Bleistein, N., 2004b, How to obtain true-amplitude common-angle gathers from one-way wave equation migration: 74th Ann. Mtg., Soc. Expl. Geophys., Expanded Abstracts, Migration 3.7.

Appendix A

The purpose of this appendix is to derive equation Equation (3), relating $d\theta'$ to dx_s. In this discussion, we can dispense with the prime on θ. To begin, we observe that

$$d\theta = \left|\frac{d\theta}{d\alpha_s}\right| d\alpha_s = \left|\frac{d\theta}{d\alpha_s}\right| \left|\frac{d\alpha_s}{dx_s}\right| dx_s. \tag{A-1}$$

As noted in the text, and as can be seen in Figure 1,

$$\left|\frac{d\theta}{d\alpha}\right| = 1. \tag{A-2}$$

The expression for the 2D Green's function WKBJ amplitude can be found in Bleistein, et al [2001], as equation (E.4.9):

$$|A(\boldsymbol{y},\boldsymbol{x})| = \frac{1}{2\sqrt{2\pi J_{2D}}}, \tag{A-3}$$

with

$$J_{2D} = \left|\frac{\partial(\boldsymbol{y})}{\partial(\sigma,\theta)}\right| = \frac{1}{v(\boldsymbol{y})}\left|\frac{\partial \boldsymbol{y}}{\partial\theta}\right|. \tag{A-4}$$

In these two equations, $\boldsymbol{y}$ is the Cartesian coordinate along the ray and σ is a standard running parameter along the ray for which

$$\frac{d\boldsymbol{y}}{d\sigma} = \boldsymbol{p} = \nabla\tau,$$

with τ the traveltime along the ray.

From Figure 2, we can see that

$$\left|\frac{\partial \boldsymbol{y}}{\partial\theta}\right| = \left|\frac{\partial x_s}{\partial\theta}\right| \cos\beta_s. \tag{A-5}$$

Now, we use this last result in the expression for J_{2D} in Equation (A-4) to obtain one expression for this function and then solve for J_{2D} in the amplitude expression, Equation

We need to carry out an integration over θ and ϕ for fixed $\hat{\boldsymbol{\nu}}$. In this case, $\boldsymbol{x}_s$ varies and we seek the Jacobian associated with the change of variables from θ and ϕ to the two nonzero coordinates of $\boldsymbol{x}_s$—x_{s1} and x_{s2}.

It is necessary to compute the 2×2 Jacobian in the identity

$$d\theta d\phi = \left|\frac{\partial(\theta, \phi)}{\partial(x_{s1}, x_{s2})}\right| dx_{s1}dx_{s2}. \tag{B-4}$$

We first use the chain rule for Jacobians to set

$$\frac{\partial(x_1, x_2)}{\partial(\theta, \phi)} = \frac{\partial(x_1, x_2)}{\partial(\alpha_{s1}, \alpha_{s2})}\frac{\partial(\alpha_{s1}, \alpha_{s2})}{\partial(\theta, \phi)} \tag{B-5}$$

The first Jacobian on the right is a cofactor of the 3D Jacobian of ray theory and therefore can be written in terms of the ray amplitude. The second Jacobian provides the scale between a differential element in $(\theta,\ \phi)$ and a differential element in the angles $(\alpha_{s1},\ \alpha_{s2})$. Below, we derive those relationships in detail.

B-1 Analysis of the first factor $\partial(x_1, x_2)/\partial(\alpha_{s1}, \alpha_{s2})$, the space-angle transformation Jacobian, in Equation (B-5).

Here we derive an expression for the first Jacobian on the right in Equation (B-5) in terms of the Green's function ray amplitude. The starting point for this derivation is equation (E.4.2) in Bleistein, et al, [2001]. In the notation of this paper, that result is

$$|A(\boldsymbol{y}, \boldsymbol{x})| = \frac{1}{4\pi}\sqrt{\frac{\sin\alpha_{s1}}{v(\boldsymbol{x})J_{3D}}}. \tag{B-6}$$

In this equation, v is the wave speed and

$$J_{3D} = \left|\frac{d\boldsymbol{y}}{d\sigma}\cdot\frac{d\boldsymbol{y}}{d\alpha_{s1}}\times\frac{d\boldsymbol{y}}{d\alpha_{s2}}\right|. \tag{B-7}$$

The variable σ is a running parameter along the ray for which

$$\frac{d\boldsymbol{y}}{d\sigma} = \boldsymbol{p} = \nabla\tau,$$

with τ the traveltime along the ray.

The cross product in Equation (B-7) is in the direction of the σ-derivative, so that

$$J_{3D} = |\nabla\tau|\left|\frac{d\boldsymbol{y}}{d\alpha_{s1}}\times\frac{d\boldsymbol{y}}{d\alpha_{s2}}\right| = \frac{1}{v(\boldsymbol{y})}\left|\frac{d\boldsymbol{y}}{d\alpha_{s1}}\times\frac{d\boldsymbol{y}}{d\alpha_{s2}}\right|. \tag{B-8}$$

The product,

$$\left|\frac{d\boldsymbol{y}}{d\alpha_{s1}}\times\frac{d\boldsymbol{y}}{d\alpha_{s2}}\right| d\alpha_{s1}d\alpha_{s2},$$

In terms of this new coordinate system, we can write

$$\hat{\boldsymbol{\alpha}}_s = \begin{bmatrix} \sin\theta\cos(\phi-\phi_0) \\ \sin\theta\sin(\phi-\phi_0) \\ \cos\theta \end{bmatrix}^T \begin{bmatrix} \boldsymbol{x}_1'' \\ \boldsymbol{x}_2'' \\ \boldsymbol{x}_3'' \end{bmatrix}. \tag{B-14}$$

In this equation and below, the superscript T denotes transpose. Further, ϕ_0 denotes a constant shift in ϕ because we do not know the orientation of the $\{''\}$ axes with respect to the zero-value of ϕ. It will not matter in the end because we will see that the Jacobian we seek is independent of $\phi - \phi_0$.

Now we need to use the transformations in Equation (B-12) and Equation (B-13) to back substitute and write a result for $\hat{\boldsymbol{\alpha}}_s$ in terms of the original coordinates where we know the representation of $\hat{\boldsymbol{\alpha}}_s$:

$$\hat{\boldsymbol{\alpha}}_s = \begin{bmatrix} \sin\theta\cos(\phi-\phi_0) \\ \sin\theta\sin(\phi-\phi_0) \\ \cos\theta \end{bmatrix}^T T_1T_2 \begin{bmatrix} \boldsymbol{x}_1 \\ \boldsymbol{x}_2 \\ \boldsymbol{x}_3 \end{bmatrix} = \begin{bmatrix} \sin\alpha_{s1}\cos\alpha_{s2} \\ \sin\alpha_{s1}\sin\alpha_{s2} \\ \cos\alpha_{s1} \end{bmatrix}^T \begin{bmatrix} \boldsymbol{x}_1 \\ \boldsymbol{x}_2 \\ \boldsymbol{x}_3 \end{bmatrix}. \tag{B-15}$$

We invert this equation to solve for $\hat{\boldsymbol{\alpha}}_s$:

$$T_2^T T_1^T \begin{bmatrix} \sin\theta\cos(\phi-\phi_0) \\ \sin\theta\sin(\phi-\phi_0) \\ \cos\theta \end{bmatrix} = \begin{bmatrix} \sin\alpha_{s1}\cos\alpha_{s2} \\ \sin\alpha_{s1}\sin\alpha_{s2} \\ \cos\alpha_{s1} \end{bmatrix} \tag{B-16}$$

Next, we need to take the derivatives of this last equation with respect to θ and ϕ. Differentiation with respect to θ leads to the equation

$$T_2^T T_1^T \begin{bmatrix} \cos\theta\cos(\phi-\phi_0) \\ \cos\theta\sin(\phi-\phi_0) \\ -\sin\theta \end{bmatrix} = \frac{\partial\alpha_{s1}}{\partial\theta} \begin{bmatrix} \cos\alpha_{s1}\cos\alpha_{s2} \\ \cos\alpha_{s1}\sin\alpha_{s2} \\ -\sin\alpha_{s1} \end{bmatrix} + \frac{\partial\alpha_{s2}}{\partial\theta} \begin{bmatrix} -\sin\alpha_{s1}\sin\alpha_{s2} \\ \sin\alpha_{s1}\cos\alpha_{s2} \\ 0 \end{bmatrix} \tag{B-17}$$

With an appropriate matrix multiply—effectively a dot product—we can solve for the two derivatives here as follows.

$$\begin{bmatrix} \cos\alpha_{s1}\cos\alpha_{s2} \\ \cos\alpha_{s1}\sin\alpha_{s2} \\ -\sin\alpha_{s1} \end{bmatrix}^T T_2^T T_1^T \begin{bmatrix} \cos\theta\cos(\phi-\phi_0) \\ \cos\theta\sin(\phi-\phi_0) \\ -\sin\theta \end{bmatrix} = \frac{\partial\alpha_{s1}}{\partial\theta}, \tag{B-18}$$

and

$$\begin{bmatrix} -\sin\alpha_{s2} \\ \cos\alpha_{s2} \\ 0 \end{bmatrix}^T T_2^T T_1^T \begin{bmatrix} \cos\theta\cos(\phi-\phi_0) \\ \cos\theta\sin(\phi-\phi_0) \\ -\sin\theta \end{bmatrix} = \sin\alpha_{s1}\frac{\partial\alpha_{s2}}{\partial\theta}. \tag{B-19}$$

Now, we repeat the process with the ϕ derivative of of the vector equality of Equation (B-16). As a first step,

$$T_2^T T_1^T \begin{bmatrix} -\sin\theta\sin(\phi-\phi_0) \\ \sin\theta\cos(\phi-\phi_0) \\ 0 \end{bmatrix} = \frac{\partial\alpha_{s1}}{\partial\phi} \begin{bmatrix} \cos\alpha_{s1}\cos\alpha_{s2} \\ \cos\alpha_{s1}\sin\alpha_{s2} \\ -\sin\alpha_{s1} \end{bmatrix} + \frac{\partial\alpha_{s2}}{\partial\phi} \begin{bmatrix} -\sin\alpha_{s1}\sin\alpha_{s2} \\ \sin\alpha_{s1}\cos\alpha_{s2} \\ 0 \end{bmatrix} \tag{B-20}$$

as an integral in source/receiver coordinates. In this appendix, we derive the Jacobian of transformation that allows us effect that change of variables, that is, to rewrite the integral in variables $\nu_1,\ \nu_2,\ \theta,\ \phi$ as an integral in the variables $x_{s1},\ x_{s2},\ x_{r1},\ x_{r2}$. As a first step, we use the chain rule for Jacobians to write

$$\frac{\partial(\nu_1,\nu_2,\theta,\phi)}{\partial(x_{s1},x_{s2},x_{r1},x_{r2})} = \frac{\partial(\alpha_{s1},\alpha_{s2},\alpha_{r1},\alpha_{r2})}{\partial(x_{s1},x_{s2},x_{r1},x_{r2})}\frac{\partial(\nu_1,\nu_2,\theta,\phi)}{\partial(\alpha_{s1},\alpha_{s2},\alpha_{r1},\alpha_{r2})}. \tag{C-1}$$

Let us consider the first factor on the right side here and observe that the direction of the ray from the source to the image point depends on the location of the source and not on the location of the receiver. Therefore, α_{s1} and α_{s2} are functions of x_{s1} and x_{s2} and not functions of x_{r1} and x_{r2}. Similarly, α_{r1} and α_{r2} are functions of x_{r1} and x_{r2} and not functions of x_{s1} and x_{s2}. Thus, the first Jacobian has the anti-diagonally 2×2 corners consisting only of zeroes and the 4×4 Jacobian is really a product of two 2×2 Jacobians, namely

$$\frac{\partial(\alpha_{s1},\alpha_{s2},\partial\alpha_{r1},\alpha_{r2})}{\partial(x_{s1},x_{s2},x_{r1},x_{r2})} = \frac{\partial(\alpha_{s1},\alpha_{s2})}{\partial(x_{s1},x_{s2})}\frac{\partial(\alpha_{r1},\alpha_{r2})}{\partial(x_{r1},x_{r2})}. \tag{C-2}$$

The first Jacobian on the right side here has been rewritten in terms of Green's function amplitudes in Appendix B, namely, as equation Equation (B-11). Of course, by replacing s by r in that fomula, we obtain the right result for the second factor. Thus,

$$\begin{aligned}\frac{\partial(\alpha_{s1},\alpha_{s2},\alpha_{r1},\alpha_{r2})}{\partial(x_{s1},x_{s2},x_{r1},x_{r2})} &= \left[16\pi^2\right]^2\frac{\cos\beta_{s1}}{\sin\alpha_{s1}}\frac{\cos\beta_{r1}}{\sin\alpha_{r1}}\frac{v(\boldsymbol{x})}{v(\boldsymbol{x}_s)}\frac{v(\boldsymbol{x})}{v(\boldsymbol{x}_r)} \\ &\quad\cdot A(\boldsymbol{x}_s,\boldsymbol{x})A^*(\boldsymbol{x}_s,\boldsymbol{x})A(\boldsymbol{x}_r,\boldsymbol{x})A^*(\boldsymbol{x}_r,\boldsymbol{x}).\end{aligned} \tag{C-3}$$

The second Jacobian on the right in equation Equation (C-1) is more complicated. A formula can be found in Burridge et al. [1998]. However, we prefer a simpler representation. Note that this expression is independent of the background model; it only depends on the transformations between various coordinate systems at the image point.

We actually calculate the inverse of the Jacobian we need for Equation (C-1). The individual elements of that Jacobian can all be calculated following the method of Appendix B. The result is surprisingly simple, namely,

$$\frac{\partial(\alpha_{s1},\alpha_{s2},\alpha_{r1},\alpha_{r2})}{\partial(\nu_1,\nu_2,\theta,\phi)} = 2\frac{\sin 2\theta\sin\nu_1}{\sin\alpha_{s1}\sin\alpha_{s2}}. \tag{C-4}$$

We combine this result with Equation (C-3), the Jacobian relating initial ray direction angles to image point angles in the expression for the Jacobian relating image point angles and source and receiver coordinates Equation (C-1) to conclude that

$$\begin{aligned}\sin\nu_1 d\nu_1 d\nu_2 d\theta d\phi &= \frac{\partial(\nu_1,\nu_2,\theta,\phi)}{\partial(x_{s1},x_{s2},x_{r1},x_{r2})}dx_{s1}dx_{s2}dx_{r1}dx_{r2} \\ &= \left[16\pi^2\right]^2\frac{\cos\beta_{s1}}{v(\boldsymbol{x}_s)}\frac{\cos\beta_{r1}}{v(\boldsymbol{x}_r)}\frac{v^2(\boldsymbol{x})}{2\sin 2\theta} \\ &\quad\cdot A(\boldsymbol{x}_s,\boldsymbol{x})A^*(\boldsymbol{x}_s,\boldsymbol{x})A(\boldsymbol{x}_r,\boldsymbol{x})A^*(\boldsymbol{x}_r,\boldsymbol{x})dx_{s1}dx_{s2}dx_{r1}dx_{r2}.\end{aligned} \tag{C-5}$$

Here, $\boldsymbol{x}_r$ is the "receiver point" at which the field is observed; $G_r(\boldsymbol{x}_r, \boldsymbol{x}', \omega)$ is the Green's function that evaluates the field at $\boldsymbol{x}_r$. It is important that the arguments be in the indicated order here. This function starts out as $G_r^\dagger(\boldsymbol{x}', \boldsymbol{x}_r, \omega)$ with † denoting "adjoint." While the acoustic wave equation with constant density is self-adjoint, that is not true in general. Thus, the Green's theorem representation of the wavefield must acknowledge the general derivation and use the Green's function of the adjoint equation. It is then a standard identity that allows us to replace the adjoint Green's function with the Green's function of the direct equation but interchanged arguments.

The next step is to replace the surface integral in the last equation above by a volume integral. Before we can do that, it is necessary to remove the normal derivative in that equation. To do so, we first use the the WKBJ approximation Equation (D-3) to rewrite the upward propagating wave representation Equation (D-4) as

$$u_R(\boldsymbol{x}_r, \boldsymbol{x}_s, \omega) \sim i\omega F(\omega) \int_S R\hat{\boldsymbol{n}} \cdot \nabla_y \tau \; G_s(\boldsymbol{x}', \boldsymbol{x}_s, \omega) G_r(\boldsymbol{x}_r, \boldsymbol{x}', \omega) dS, \qquad \tau = \tau_s + \tau_r. \tag{D-5}$$

Now, we further simplify this result by observing that at the stationary point(s) of the integration, $\hat{\boldsymbol{n}}$ and $\nabla_y \tau$ are co-linear but point in opposite directions:

$$\hat{\boldsymbol{n}} \cdot \nabla_{x'} \tau = -|\nabla_{x'} \tau|. \tag{D-6}$$

Therefore, we can rewrite Equation (D-5) as

$$u_R(\boldsymbol{x}_r, \boldsymbol{x}_s, \omega) \sim -i\omega F(\omega) \int_S R|\nabla_{x'} \tau| G_s(\boldsymbol{x}', \boldsymbol{x}_s, \omega) G_r(\boldsymbol{x}_r, \boldsymbol{x}', \omega) dS. \tag{D-7}$$

Next, we introduce the *singular function* of the reflection surface denoted by $\gamma(\boldsymbol{x}')$ in Bleistein et al [2001]. This is a delta function of normal distance to the surface. Further, the product $R\gamma$ is what we mean by the *reflectivity* function denoted by $\mathcal{R}(\boldsymbol{x}')$. What matters to us here is that $dndS = dV$ and $\int\{\cdot\}\gamma dV = \int\{\cdot\}dS$; that is, the introduction of $\gamma\; dn$ and another integration transforms the surface integral into a volume integral in the variables, $\boldsymbol{x}'$.

The second representation of the upward propagating wave Equation (D-4) is now recast as Equation (18).

Appendix E: Asymptotic analysis of the norm $\|(K^\dagger K)^{-1}\|$.

We describe the asymptotic analysis of the operator norm Equation (22) in this appendix. First, we replace the Green's functions by their ray-theoretic equivalents. Then, Equation (22) becomes

$$\begin{aligned} \|(K^\dagger K)^{-1}\| \;=\; \Big| \int d^2\xi d\omega \int dV \omega^2 |\nabla_{x'} \tau(\boldsymbol{x}', \boldsymbol{\xi})| A_s^*(\boldsymbol{x}_s, \boldsymbol{x}) A_r^*(\boldsymbol{x}, \boldsymbol{x}_r) \\ \cdot |\nabla_x \tau(\boldsymbol{x}, \boldsymbol{\xi})| A_s(\boldsymbol{x}', \boldsymbol{x}_s) A_r(\boldsymbol{x}_r, \boldsymbol{x}') e^{i\omega\{\tau(\boldsymbol{x}', \boldsymbol{\xi}) - \tau(\boldsymbol{x}, \boldsymbol{\xi})\}} \Big|^{-1}, \end{aligned} \tag{E-1}$$

independent of the KMAH index.

Equation (E-1) becomes

$$\|(K^\dagger K)^{-1}\| = \left| \int d^3k \int dV \left| \nabla_{\boldsymbol{x}}\tau(\boldsymbol{x},\boldsymbol{\xi}) | A_s(\boldsymbol{x},\boldsymbol{x}_s) A_r(\boldsymbol{x}_r,\boldsymbol{x}) \right|^2 \omega^2 \left| \frac{\partial(\boldsymbol{\xi},\omega)}{\partial(\boldsymbol{k})} \right| e^{i\boldsymbol{k}\cdot(\boldsymbol{x}'-\boldsymbol{x})} \right\} \right|^{-1}. \tag{E-3}$$

It is easier to write down the inverse of the Jacobian of transformation from the variables $\boldsymbol{\xi},\omega$ to $\boldsymbol{k}$ than to calculate the indicated Jacobian under the integral sign here. For that purpose, we use the definition of $\boldsymbol{k}$ in Equation (E-2). The result is

$$\frac{\partial(\boldsymbol{k})}{\partial(\boldsymbol{\xi},\omega)} = \omega^2 \det \begin{bmatrix} \nabla_{\boldsymbol{x}}\tau(\boldsymbol{x},\boldsymbol{\xi}) \\ \\ \dfrac{\partial \nabla_{\boldsymbol{x}}\tau(\boldsymbol{x},\boldsymbol{\xi})}{\partial \xi_1} \\ \\ \dfrac{\partial \nabla_{\boldsymbol{x}}\tau(\boldsymbol{x},\boldsymbol{\xi})}{\partial \xi_2} \end{bmatrix} = \omega^2 h(\boldsymbol{x},\boldsymbol{\xi}). \tag{E-4}$$

In this equation $h(\boldsymbol{x},\boldsymbol{\xi})$ is the usual Beylkin determinant.

Using this result in norm representation Equation (E-3) leads to the result

$$\|(K^\dagger K)^{-1}\| = \left| \int d^3k \int dV \left| \nabla_{\boldsymbol{x}}\tau(\boldsymbol{x},\boldsymbol{\xi}) | A_s(\boldsymbol{x},\boldsymbol{x}_s) A_r(\boldsymbol{x}_r,\boldsymbol{x}) \right|^2 |h(\boldsymbol{x},\boldsymbol{\xi})|^{-1} e^{i\boldsymbol{k}\cdot(\boldsymbol{x}'-\boldsymbol{x})} \right\} \right|^{-1}. \tag{E-5}$$

In this integral, note that ω appears in the phase in $\boldsymbol{k}$, but no longer appears in the amplitude, which then is a function of $\boldsymbol{\xi}(\boldsymbol{k})$. It is a remarkable fact of the change of variables defined in Equation (E-2) that, except for sign(ω), $\boldsymbol{\xi}$ is a function of the direction of $\boldsymbol{k}$ and independent of its magnitude. To see this, simply divide $\boldsymbol{k}$ in Equation (E-2) by its magnitude to determine that

$$\hat{\boldsymbol{k}} = \frac{\boldsymbol{k}}{|\boldsymbol{k}|} = \text{sign}(\omega) \frac{\nabla_{\boldsymbol{x}}\tau(\boldsymbol{x},\boldsymbol{\xi})}{|\nabla_{\boldsymbol{x}}\tau(\boldsymbol{x},\boldsymbol{\xi})|} = \text{sign}(\omega)\hat{\boldsymbol{\nu}}, \tag{E-6}$$

with $\hat{\boldsymbol{\nu}}$ defined in Figure 3. Both choices of $\hat{\boldsymbol{k}}$ are attached to the same migration dip, hence, the same $\boldsymbol{\xi}$; so sign(ω) has no effect on the amplitude of the integrand in Equation (E-5), our last expression for the norm we seek. Consequently, the only dependence on $k = |\boldsymbol{k}|$ in the integrand is in the phase. This suggests that we would be better off analyzing this integral in spherical-polar coordinates. We introduce k and two spherical-polar angles, ν_1 and ν_2, with ν_1 measured from the line defined by $\boldsymbol{x}' - \boldsymbol{x}$. In this case,

$$d^3k = k^2 \sin\nu_1 d\nu_1 d\nu_2 dk,$$

and the k-domain integration in the norm representation, Equation (E-5), takes the form

$$\int d^3k \cdots e^{i\boldsymbol{k}\cdot(\boldsymbol{x}'-\boldsymbol{x})} = \int k^2 \sin\nu_1 d\nu_1 d\nu_2 dk \cdots e^{ik|\boldsymbol{x}'-\boldsymbol{x}|\cos\nu_1}. \tag{E-7}$$

equation Equation (E-4). Note that the three rows of the matrix whose determinant is to be calculated are merely the gradient of the travel time and its derivatives with respect to the coordinates that describe the source/receiver array. Let us rewrite that gradient as a product of its magnitude and unit direction vector:

$$\nabla_x \tau(\boldsymbol{x}, \boldsymbol{\xi}) = \frac{2\cos\theta}{v(\boldsymbol{x})}\hat{\boldsymbol{\nu}} \tag{F-1}$$

The magnitude stated here is derived in Bleistein, et al, [2001], equation (5.1.45). When we differentiate this product, there is one term that is proportional to $\hat{\boldsymbol{\nu}}$ and one that is not. In calculating the determinant, we can neglect the portion of the second and third rows that are proportional to $\hat{\boldsymbol{\nu}}$, because they are in the same direction as the entire first row. Therefore,

$$h(\boldsymbol{x}, \boldsymbol{\xi}) = \det \begin{bmatrix} \dfrac{2\cos\theta}{v(\boldsymbol{x})}\hat{\boldsymbol{\nu}} \\[2ex] \dfrac{2\cos\theta}{v(\boldsymbol{x})}\dfrac{\partial\hat{\boldsymbol{\nu}}}{\partial\xi_1} \\[2ex] \dfrac{2\cos\theta}{v(\boldsymbol{x})}\dfrac{\partial\hat{\boldsymbol{\nu}}}{\partial\xi_2} \end{bmatrix} = \left[\frac{2\cos\theta}{v(\boldsymbol{x})}\right]^3 \det \begin{bmatrix} \hat{\boldsymbol{\nu}} \\[2ex] \dfrac{\partial\hat{\boldsymbol{\nu}}}{\partial\xi_1} \\[2ex] \dfrac{\partial\hat{\boldsymbol{\nu}}}{\partial\xi_2} \end{bmatrix}. \tag{F-2}$$

Since $\hat{\boldsymbol{\nu}}$ is a unit vector, its derivatives with respect to ξ_1 and ξ_2 are both orthogonal to the vector $\hat{\boldsymbol{\nu}}$. Thus, if we think of this determinant as a triple scalar product, the cross-product of the last two rows are colinear with $\hat{\boldsymbol{\nu}}$ and we can write

$$h(\boldsymbol{x}, \boldsymbol{\xi}) = \left[\frac{2\cos\theta}{v(\boldsymbol{x})}\right]^3 \left|\frac{\partial\hat{\boldsymbol{\nu}}}{\partial\xi_1} \times \frac{\partial\hat{\boldsymbol{\nu}}}{\partial\xi_2}\right|. \tag{F-3}$$

Hence, within a sign we obtain the result Equation (27) for the Beylkin determinant divide by the magnitude of the gradient of traveltime. Since we require the absolute value for the Jacobian of coordinate transformation, the sign ambiguity is of no consequence.

We can also see from this last expression for the Beylkin determinant in Equation (F-3) where the difficulty arises in computing the Beylkin determinant when (ξ_1, ξ_2) are parameters on the acquisition surface. The connection via rays, especially for the case of common-offset data, is particularly difficult to compute. On the other hand, when the integration parameters that we use are the spherical polar coordinates of $\boldsymbol{k}$ at the image point, the cross produce appearing in Equation (F-3) is just $\sin\nu_1$. If we were to use cylindrical coordinates for $\hat{\boldsymbol{\nu}}$, then the cross product is just equal to one!

Equation (F-3) is the most concise representation of the Beylkin determinant in 3D.